

Creation of 3D Volume Loss Mask and Mean Performance Analysis on 3d MR Images

¹Muhammet Üsame ÖZİÇ, ²Ahmet Hakan EKMEKÇİ, ¹Seral ÖZŞEN

¹Department of Electrical- Electronics Engineering, Selcuk University, Konya, TURKEY;

²Department of Neurology, Selcuk University, Konya, TURKEY;

muozic@selcuk.edu.tr; hakanekmekci@selcuk.edu.tr; seral@selcuk.edu.tr

ABSTRACT

Examination of changes in the brain during disease progression using numerical methods is one of the current topics investigated by neuroscience. One of the numerical methods developed for locally or globally analyzing changes in the brain is voxel based morphometry. With voxel based morphometry, volume differences between the intragroup and intergroup Magnetic Resonance images can be examined. The general voxel based morphometry studies performed in the literature are only mapped. However, tissue analysis and artificial intelligence studies using voxel based morphometry are inadequate. In this study, voxel based morphometry was used to create a three dimensional volume loss mask for Alzheimer's disease to use tissue analysis and artificial intelligence in the future studies. Two different masks were created for according to the usage of family wise error. Volume loss regions are cut from normalized segmented and smoothed normalized segmented gray matter images with the generated masks. The average values of the voxel values in these regions are statistically compared for four different scenarios. As a result of the comparison, segmentation made with normalized segmented and family wise error values have been more meaningful results than the other three scenarios.

Keywords: Voxel based morphometry; Alzheimer; Family wise error; Volume loss mask; Masking

1 Introduction

Computational neuroanatomy is a neuroscience branch that scientists have searched for many years and many researches still continue [1]. In particular, which regions of the brain are central to which functions in the body and the determination of non-invasive measurements of these regions by digital sources is important both in terms of tracking the disease progression and capturing in the early stage of the disease. Some of the issues of computational neuroanatomy include tracking of any atrophy in the brain, size of damage, local and global morphometry changes, shape and volume changes in cortical regions of the brain, tracking of tumor and lesion formation, connectivity analysis, tractography, signal analysis. Early studies on neuroanatomy started manually with brain autopsy. Later on, with the development of imaging methods, it became possible to quantitatively evaluate the brain activities that required digital sources [2] [3].

DOI: 10.14738/jbemi.43.3237

Publication Date: 30th June 2017

URL: <http://dx.doi.org/10.14738/jbemi.43.3237>

Voxel Based Morphometry (VBM) is one of popular methods developed for monitoring intergroup-intragroup differences on cross-sectional and longitudinal 3D magnetic resonance (MR) images. VBM is a statistical evaluation of voxel based changes after applying some preprocessing on images [4]. As a result of the process, the differences between the images can be easily mapped on a common atlas so that the region in which the change is located can be easily tracked[5-7].

Analyzing the whole image in artificial intelligence studies made with 3D MR images creates problems in terms of time and data size. It is obvious that looking at the region of interest (ROI) instead of analyzing the whole image will give fast and accurate results. In this study, it was investigated how to use VBM method for ROI analysis in three dimensional MR images. It is a preliminary study for decision support systems and 3D MR classification to be used VBM masks. Firstly, we will examine in detail how to construct a three dimensional ROI mask using the VBM method. The gray matter (GM) changes between the MR images of the Alzheimer's Disease (AD) and Normal Control (NC) groups taken from the Open Access Series of Imaging Studies (OASIS) database [8] will be examined by VBM method and three dimensional volume loss masks will be created. The loss masks can be produced in two ways with and without Family Wise Error (FWE). This value is often used to eliminate false positive results [9, 10] . But, some studies use this value while others do not. The effect of this value on the study results will be examined statistically. Secondly, GM images are masked in three dimensions with the loss masks obtained. But, there are some contradicts at this stage. Two different GM images are produced in normalize space. Normalized image preserving texture information and modulated image preserving volume information are obtained after normalization [4]. Normalized imaged which preserves texture information were used in this study because it is stated that the mezosopic differences show better with respect to modulated normalized images [11, 12]. However, in some studies normalized images have been made smoothing for artificial intelligence studies [13] . At this time, valuable tissue information may be lost. Four different scenarios have been tested in this study to examine these different approaches. Masking process was made for normalized image with FWE, normalized image without FWE, smoothed normalized image with FWE, smoothed normalized image without FWE. The differences between AD and NC were examined by independent samples t-test by taking the average of voxel values under the VBM masks for these four scenarios. The aim of this assessment is a preliminary study of which scenario might be better for future artificial intelligence and decision support system studies. SPM8, VBM8 and MRICro package programs were used in the study.

2 Voxel Based Morphometry

Morphology is a science that examines the formal differences or similarities that occur in living and non-living beings. In brain research, morphometry examines the anatomical structure of the brain locally or globally [14, 15]. Manual measurement of the brain morphometry being used today is only possible after the patient's brain death. With the development of non-invasive imaging techniques such as MR imaging, high level programs and morphometry analysis have been developed by neuroscientists and engineers [16]. Although there are many programs for this purpose, three programs commonly used in the literature are MATLAB-based Statistical Parametric Mapping (SPM) [17], linux operating system based FSL [18] developed at Oxford University, and linux based Freesurfer programs developed at Harvard University [19]. The SPM8 (<http://www.fil.ion.ucl.ac.uk/spm/software/spm8/>) version was used in our work provides a comprehensive library for preprocessing, segmentation and statistical analysis in MR images. The SPM8 version can also perform fMRI, PET and EEG analyzes besides MR

images [20]. Researchers can use the program library to create customized new tools and they release them to the world's researchers from the SPM8 website. The VBM8 (<http://dbm.neuro.uni-jena.de/vbm8/>) library, one of these customized tools, allows the preprocessing steps for VBM to be carried out on an interface, allowing them to be done quickly [21]. Developed by a team at Jena University, the VBM8 library can be run by copying into the toolbox file named in the SPM8 folders. The raw MR image given to the VBM8 tool is preprocessed in the direction of the inputs given by the user and made ready for VBM analysis. The segmented regions of the three main brain regions, Gray Matter (GM), White Matter (WM), Cerebrospinal Fluid (CSF), are output in both normal space and normalized tissue probability map space. During the construction of these operations, the basic two types of noise in MR images, random noise and bias noise, are automatically cleaned. An adaptive filter is needed because noises of MR images come from random sources that affect the image during image acquisition. For this purpose, the Spatial Adaptive Non Local Means Filter has been added to the VBM8 library and can be used practically [22]. At the same time, the bias noise originating from the magnetic field is eliminated by combining the basic functions of the discrete cosine transformation [23].

3 Material and Methods

3.1 Data

The data used in the study were taken from the OASIS database (<http://www.oasis-brains.org>). There are 416 data in the database and there are subjects in different age ranges from young population to elderly population. Because the study was concerned with AD, 70 patients and 70 normal MR images labeled with Clinical Dementia Rating (CDR) over 65 years of age were included in the study. CDR is a psychological test used to measure the severity of a disease in AD. CDR consists of five stages as CDR0: Normal, CDR0.5: Mild Cognitive Impairment, CDR1: Mild Stage, CDR2: Moderate Stage, CDR3: Severe Stage in Alzheimer [8]. The population of subjects was formed after the covariance analysis with "Quality control of data with covariance boxplot" tool of the VBM8 and the age average cohort. The data for the population of the study are given in Table 1. (MMSE=Mini Mental State Examination)

Table 1. Demographic features used data

NC					
Age Gr.	Numb.	M\F	Mean Age	Mean MMSE	CDR
60s	9	3\6	68.00±1.11	28.77±1.64	0
70s	32	8\24	73.37±2.44	29.15±0.91	0
80s	22	6\16	83.40±3.27	28.77±1.26	0
90s	7	1\6	91.14±1.67	28.57±1.71	0
Total	70	18\52	77.61±7.48	28.92± 1.21	0

AD					
Age Gr.	Numb.	M\F	Mean Age	Mean MMSE	CDR
60s	7	3\4	67.85± 1.21	23.42± 4.85	5\2\0
70s	35	14\21	74.42±2.61	24.54±4.21	23\11\1
80s	23	11\12	82.69± 2.61	24.47 ±4.06	16\6\1
90s	5	2\3	92.00± 2.44	23.80±1.92	4\1\0
Total	70	30\40	77.74 ±6.66	24.35 ±4.05	48\20\2

AD starts with old age and moves secretly in the brain. The main brain markers of the disease are volume loss in the temporal lobe and limbic system that parts of gray matter, symmetry deterioration, lateral ventricular enlargement, brain shrinkage, tissue degeneration like as senile plaque and neurofibrillary tangles [24]. In Figure 1, NC and AD images clearly show the main brain markers of the disease.

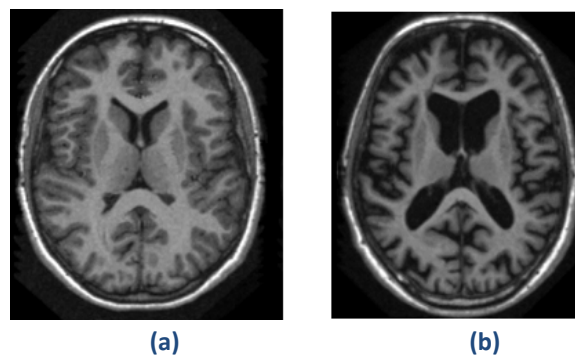


Figure 1 (a) Normal (b) Alzheimer

Imaging protocols are TR= 9.7 msn, TE= 4.0 msn., flip angle= 10, TI= 20 msn, TD= 200 msn, sagittal orientation, slice thickness 1.25 mm without gap , resolution 1x1 mm, 256x256 matrix size, 1.5T T1 weighted Magnetization-Prepared Rapid Gradient Echo (MP-RAGE) and siemens MRI device. There are raw images and Talairach axis-registered images in the database. At the same time, some preprocessings are already made in the data. However, it is thought that for the VBM, the Talairach axis-registered images may cause data loss after registering to the Montreal Neurological Institute (MNI) space. For this reason, any unprocessed raw MR images with the size of 256*256*160, 1*1*1 voxel size prefixed with "OAS1_xxxx_MrY_mpr_ni_anon_sbj_111" in the study were used.

3.2 Preprocessing

Here are the preprocessing steps for the VBM technique on the data we have taken from the OASIS database.

- 1) Images were converted from sagittal plane to axial plane using MRICro program.
- 2) Because of the axial shifts in the MR images, MATLAB gave errors when running the VBM8 library. For this reason, each MR image was manually corrected by reorienting so that anterior commissure(AC)/posterior commissure(PC) plane was to be AC (x, y, z)= 0.
- 3) The basic noise reduction parameters in the VBM8 library were taken default. Random noise and bias noise were eliminated.

4)The VBM8 library gives two different segmentation outputs as modulated and unmodulated. While modulated images preserve volume after normalization, unmodulated images preserve tissue concentration [4]. It is stated in studies that unmodulated images give better accuracy for classification and that mesoscopic differences can be better distinguished than modulated images[11] [12]. However, some classification studies use modulated normalized images [13, 25]. In this work, GM output of the VBM8 was set to be unmodulated normalized according to [12].

5)The VBM8 library offers two different normalization methods: "Low-dimensional: SPM Default" and "High Dimensional:Dartel".Diffeomorphic Anatomical Registration Through Exponentiated Lie Algebra (DARTEL) is the normalization technique that used a diffeomorphic framework developed by John Ashburner [26]. The DARTEL method has been used in our study because of the high level of registration in experiments with different normalization methods and high performance in the registration of MR data obtained in different imaging protocols in multiple center studies [27, 28].

6) GM images were smoothed with 8mm [full width at half maximum](#) (FWHM) low pass gauss filter. The aim here is to smooth reducing the voxel values that will affect negatively on the analysis result and to increase the statistical power [21].

7) With the "Check sample homogeneity using covariance" tool found under the VBM8 library, some data have been removed from studies that are caused by errors in segmentation and normalization.

The necessary preprocessing steps for the raw MR images was performed one by one and it is shown in Figure 2 over the subject of OASIS 028. The outliers in the covariance boxplot graph shown in Figure 2 were omitted from the study. Subjects over 65 years of age were included in the study. 70 AD and 70 NC groups were established to take into account age compatibility.

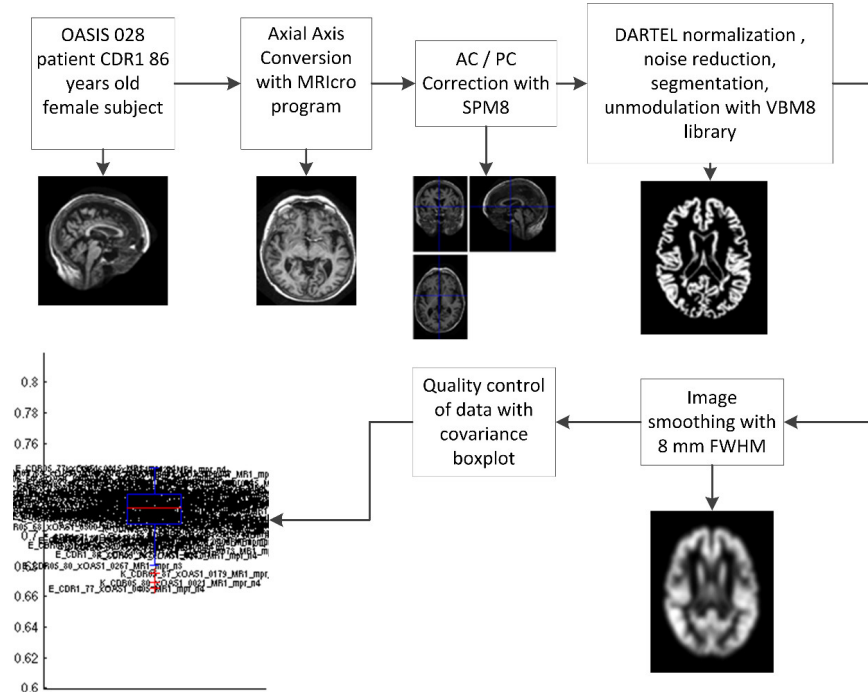


Figure 2 Flowchart of MR image preprocessing

3.3 Experimental Design Matrix

After the preprocessing steps, it is necessary to estimate the experimental parameters. If the data are considered as a whole, covariates that may adversely affect the experimental results must be taken into account. The steps required to estimate the test parameters are listed below.

- 1) "Specify 2nd-level" is selected in SPM8 program to create experiment design. "Two sample t-test" are chosen because there are two groups in this study as AD and NC.
- 2) Age, TIV, sex are entered as covariate.
- 3) Experimental parameters are estimated with the generated "SPM.mat" file.
- 4) The t-contrasts of the groups to be compared with the "SPM.mat" file are created as AD > NC and AD < NC.
- 5) Other parameters are "apply masking": none, "Threshold {T or p value}x": 0.001, extent threshold {voxels}: 0. These parameters are taken as default.
- 6) FWE=0.05 or not
- 7) By pressing the button "hot map", the three dimensional volume mask named "hot.img" can be easily created.

After preprocessing and experimental design, the glass brain images obtained according to the family wise error are given in Figure 3. Figure 3 shows (a) glass brain without FWE, (b) glass brain with FWE, and (c) experimental design matrix.

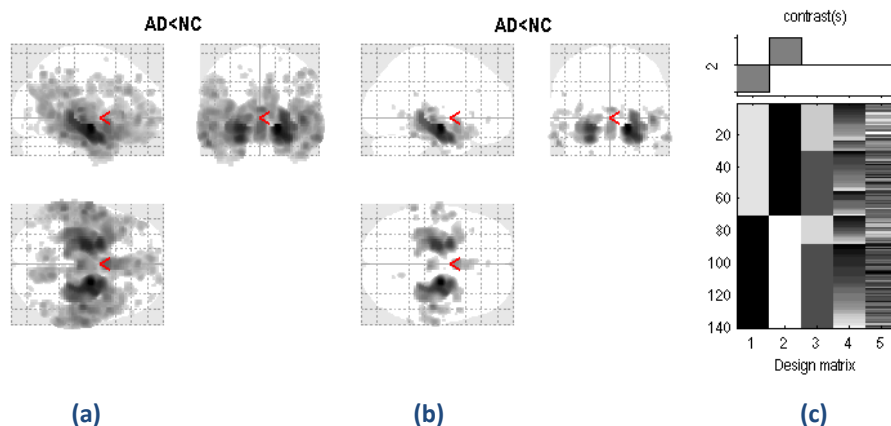


Figure 3 (a) Glass brain without FWE (b) Glass brain with FWE (c) Experimental Design Matrix

As seen in Figure 3, differences in the brain between AD and NC are clearly seen in the temporal lobe and limbic lobe regions. These differences are consistent with the volume losses seen in the literature. The use of the FWE reduces false positive voxel in the glass brain. After the glass brains were obtained, masks were created with the "hot map" key. These masks were assigned to all voxels greater than 0 by a simple script created with MATLAB. Two different masks as FWE and without FWE were created by using glass brain. With these masks, normalized GM and smoothed normalized GM were segmented by masked ROIs. By taking the average of the voxel intensity values found in the obtained volume loss regions, 4 different scenarios were produced for each group of subjects. Figure 4 shows (a) Normalized segmented GM, (b) 3D binary mask without FWE, (c) Superimposing normalized segmented and binary mask, (d) Cutting of the region under the mask, (e) Normalized segmented smoothed GM, (f) 3D binary mask without FWE, (g) Superimposing normalized segmented smoothed and binary mask (h), Cutting of

the region under the mask. Figure 5 shows (a) Normalized segmented GM, (b) 3D binary mask with FWE, (c) Superimposing normalized segmented and binary mask, (d) Cutting of the region under the mask, (e) Normalized segmented smoothed GM, (f) 3D binary mask with FWE, (g) Superimposing normalized segmented smoothed and binary mask, (h) Cutting of the region under the mask. Figure 6 shows (a) Boxplot with FWE masked normalized segmented GM between AD and NC, (b) Boxplot without FWE masked normalized segmented GM between AD and NC, (c) Boxplot with FWE masked normalized segmented smoothed GM between AD and NC, (d) Boxplot with FWE masked normalized segmented smoothed GM between AD and NC.

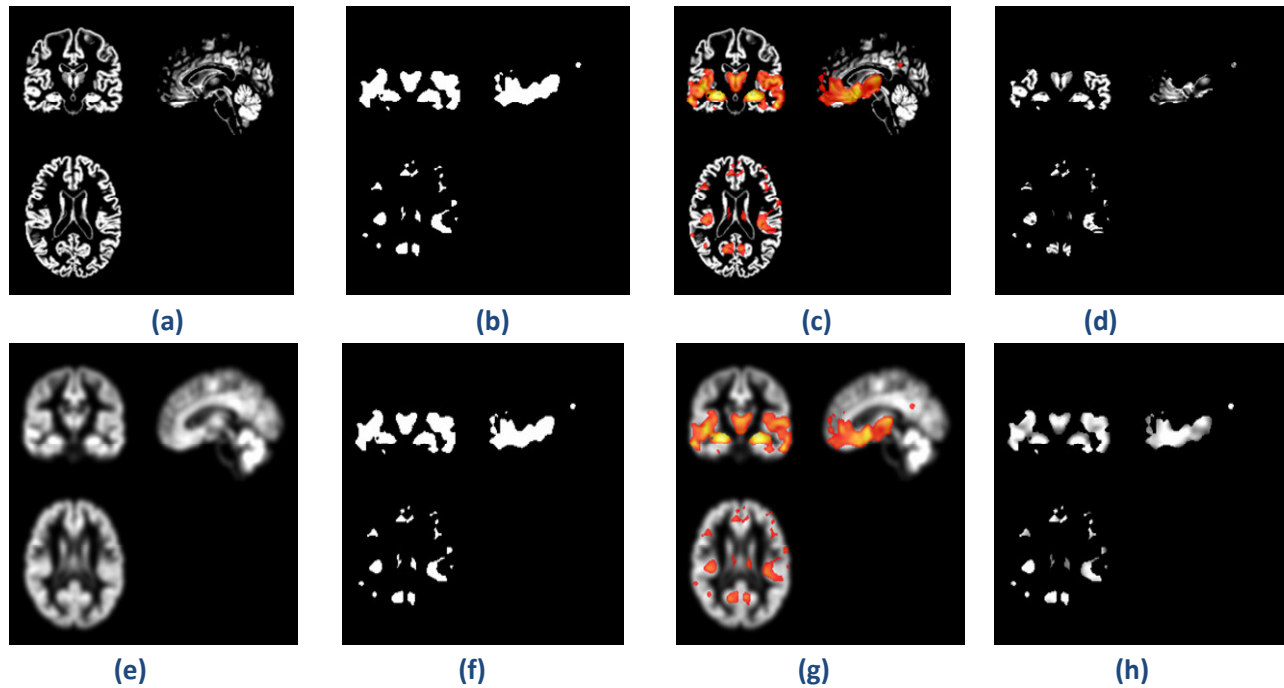


Figure 4 (a) Normalized segmented GM (b) 3D binary mask without FWE (c) Superimposing normalized segmented and binary mask (d) Cutting of the region under the mask (e) Normalized segmented smoothed GM (f) 3D binary mask without FWE (g) Superimposing normalized segmented smoothed and binary mask (h) Cutting of the region under the mask

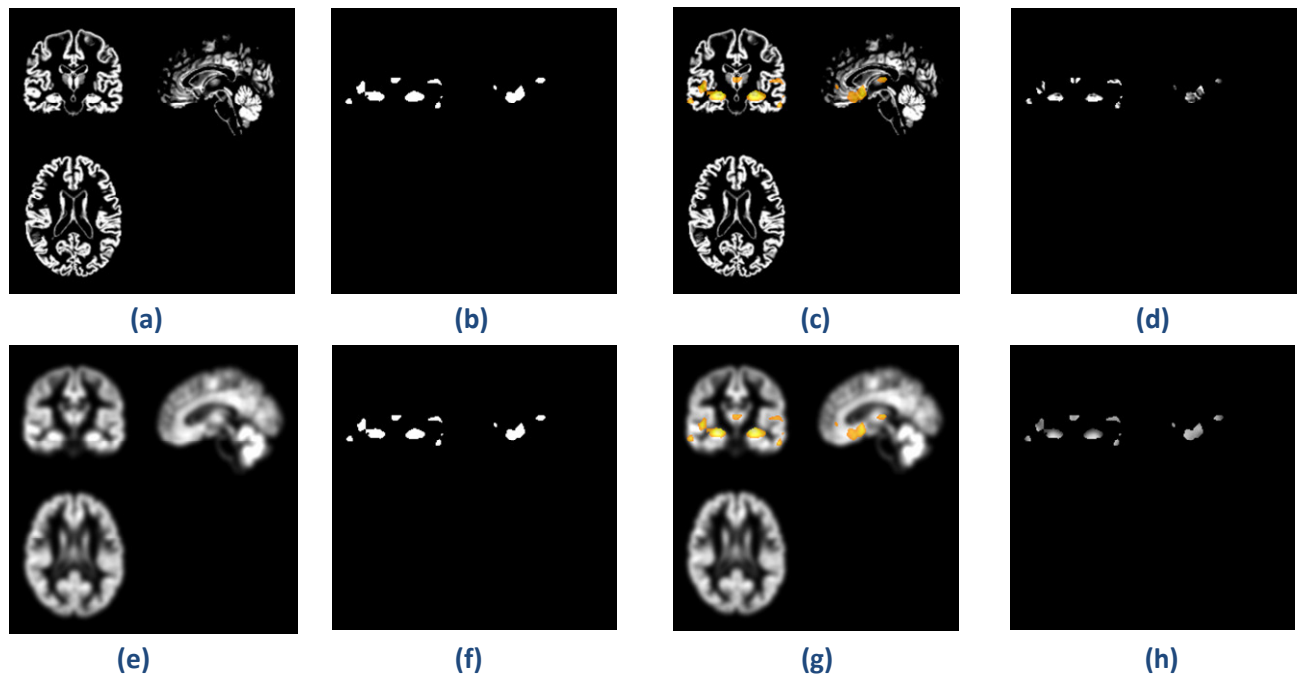


Figure 5 (a) Normalized segmented GM (b) 3D binary mask with FWE (c) Superimposing normalized segmented and binary mask (d) Cutting of the region under the mask (e) Normalized segmented smoothed GM (f) 3D binary mask with FWE (g) Superimposing normalized segmented smoothed and binary mask (h) Cutting of the region under the mask

4 Conclusion

In this study, two volume loss masks for Alzheimer's disease were produced according to the usage of FWE with VBM method. With the two 3D binary masks created, normalized segmented GM and smoothed normalized segmented GM images were cut from the corresponding regions. By taking the average of voxel values in these regions, statistical analysis was performed for four different scenarios between normal and patient groups using MATLAB statistical tool. As shown in Table 2, mean values are statistically significant according to t-test for all scenarios between patient and normal. (NGM=Normalized Segmented Gray Matter, SNGM=Smoothed Normalized Gray Matter)

Table 2. Statistical Results of mean values remaining under ROI masks for four different scenarios

	AD		NC		Stats
	Mean	Std	Mean	Std	p
NGM-With FWE	0.49	0.047	0.558	0.036	2.15E-17
NGM-Without FWE	0.522	0.031	0.568	0.025	2.59E-17
SNGM-With FWE	0.463	0.038	0.514	0.029	2.05E-15
SNGM-Without FWE	0.463	0.027	0.498	0.022	3.35E-14

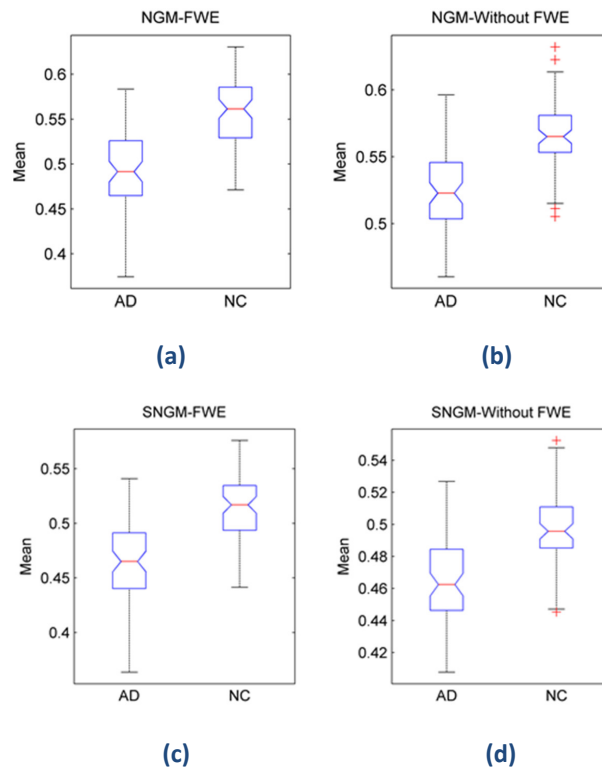


Figure 6 (a) Boxplot with FWE masked normalized segmented GM between AD and NC (b) Boxplot without FWE masked normalized segmented GM between AD and NC (c) Boxplot with FWE masked normalized segmented smoothed GM between AD and NC (d) Boxplot without FWE masked normalized segmented smoothed GM between AD and NC

Calculations made with masks created using FWE have more meaningful results than calculations made with masks created without using FWE. Normalized segmented GM images produced more meaningful results than normalized segmented smoothed images regardless of FWE value. Among the four different scenarios performed, the most significant result was seen with mask obtained using FWE and normalized segmented GM images. In AD, instead of the volumetric losses that began on GM, cerebrospinal fluid come in, thus increasing pattern variation occurs in volume loss regions. The voxel colors in the corresponding regions convert from whitish to black. Thus, the voxel values and voxel intensities in the regions below of the loss masks will be reduced relative to the normal subjects. From this point of view, it is reasonable that the mean value differences of the areas under the mask are significant between patient and control as seen Table 2. It has been determined in this study that calculations made with the FWE value, which reduces false positive results, give more precise results. Smoothed operations on segmented images are usually done at the VBM step. This process is to increase the statistical power by smoothing the defective voxels occurred segmentation phase. However, when looking at the masked regions, the average values appear to be more meaningful in non-smoothed images. Smoothed images can be useful for increasing statistical power and for eliminating false voxel values resulting from segmentation, but it was appeared that the region that underlies the ROI in terms of average changes of the voxel values, making it less meaningful in determining the pattern. As shown in the boxplot graphs given in Figure 6, the median values are higher in the normal groups in 4 different scenarios. However, images that do not use FWE show outliers. According to the boxplot charts, there are no outliers in the scenario made with FWE. It has been found

that using the FWE value in the VBM process gives more meaningful results. Smoothed normalized images have been shown to be more meaningless results when determining volume loss regions than non-smoothed normalized images.

It is clear that instead of looking at the whole of the MR images, only looking at the differences in the relevant regions will give more precise results in cross-sectional and longitudinal studies. The pattern change generated by the voxel values in the corresponding regions can give fast and practical results for the early stage diagnosis of the disease. In future work, the performance of classifying of voxel values in volume loss regions with masks by using artificial intelligence methods and machine learning techniques will be investigated for more different scenarios.

REFERENCES

- [1]. Ascoli, G.A., Computational neuroanatomy: Principles and methods 2002: Springer Science & Business Media.
- [2]. Weiskopf, N., et al., Advances in MRI-based computational neuroanatomy: from morphometry to in-vivo histology. *Current opinion in neurology*, 2015. 28(4): p. 313-322.
- [3]. Ashburner, J., et al., Computer-assisted imaging to assess brain structure in healthy and diseased brains. *The Lancet Neurology*, 2003. 2(2): p. 79-88.
- [4]. Mechelli, A., et al., Voxel-based morphometry of the human brain: methods and applications. *Current medical Imaging reviews*, 2005. 1(2): p. 105-113.
- [5]. Baron, J., et al., In vivo mapping of gray matter loss with voxel-based morphometry in mild Alzheimer's disease. *Neuroimage*, 2001. 14(2): p. 298-309.
- [6]. Chetelat, G., et al., Mapping gray matter loss with voxel-based morphometry in mild cognitive impairment. *Neuroreport*, 2002. 13(15): p. 1939-1943.
- [7]. Chetelat, G., et al., Using voxel-based morphometry to map the structural changes associated with rapid conversion in MCI: a longitudinal MRI study. *Neuroimage*, 2005. 27(4): p. 934-946.
- [8]. Marcus, D.S., et al., Open Access Series of Imaging Studies (OASIS): cross-sectional MRI data in young, middle aged, nondemented, and demented older adults. *Journal of cognitive neuroscience*, 2007. 19(9): p. 1498-1507.
- [9]. Glickman, M.E., S.R. Rao, and M.R. Schultz, False discovery rate control is a recommended alternative to Bonferroni-type adjustments in health studies. *Journal of clinical epidemiology*, 2014. 67(8): p. 850-857
- [10]. Nichols, T. and S. Hayasaka, Controlling the familywise error rate in functional neuroimaging: a comparative review. *Statistical methods in medical research*, 2003. 12(5): p. 419-446.
- [11]. Dashjants, T., et al., Alzheimer's disease: diagnosis by different methods of voxel-based morphometry. *Fukuoka Igaku Zasshi*, 2012. 103(3): p. 59-69.

- [12]. Radua, J., et al., Validity of modulation and optimal settings for advanced voxel-based morphometry. *Neuroimage*, 2014. 86: p. 81-90.
- [13]. Aggarwal, N., B. Rana, and R. Agrawal, 3d discrete wavelet transform for computer aided diagnosis of Alzheimer's disease using t1-weighted brain MRI. *International Journal of Imaging Systems and Technology*, 2015. 25(2): p. 179-190.
- [14]. Pfefferbaum, A., et al., A quantitative magnetic resonance imaging study of changes in brain morphology from infancy to late adulthood. *Archives of neurology*, 1994. 51(9): p. 874-887.
- [15]. Hu, H.-H., et al., Shape and curvedness analysis of brain morphology using human fetal magnetic resonance images in utero. *Brain Structure and Function*, 2013. 218(6): p. 1451-1462.
- [16]. Keller, S.S. and N. Roberts, Measurement of brain volume using MRI: software, techniques, choices and prerequisites. *J Anthropol Sci*, 2009. 87: p. 127-151.
- [17]. Penny, W.D., et al., *Statistical parametric mapping: the analysis of functional brain images 2011*: Academic press.
- [18]. Jenkinson, M., et al., *Fsl. Neuroimage*, 2012. 62(2): p. 782-790.
- [19]. Fischl, B., *FreeSurfer. Neuroimage*, 2012. 62(2): p. 774-781.
- [20]. Ashburner, J., et al., *SPM8 manual. Functional Imaging Laboratory, Institute of Neurology*, 2008: p. 41.
- [21]. Kurth, F., E. Luders, and C. Gaser, *VBM8 toolbox manual. Jena: University of Jena*, 2010.
- [22]. Manjón, J.V., et al., Adaptive non-local means denoising of MR images with spatially varying noise levels. *Journal of Magnetic Resonance Imaging*, 2010. 31(1): p. 192-203.
- [23]. Myronenko, A. and X. Song, Intensity-based image registration by minimizing residual complexity. *IEEE Transactions on Medical Imaging*, 2010. 29(11): p. 1882-1891.
- [24]. Vemuri, P. and C.R. Jack, Role of structural MRI in Alzheimer's disease. *Alzheimer's research & therapy*, 2010. 2(4): p. 23.
- [25]. Savio, A., et al., Neurocognitive disorder detection based on feature vectors extracted from VBM analysis of structural MRI. *Computers in biology and medicine*, 2011. 41(8): p. 600-610.
- [26]. Ashburner, J., A fast diffeomorphic image registration algorithm. *Neuroimage*, 2007. 38(1): p. 95-113.
- [27]. Goto, M., et al., Diffeomorphic Anatomical Registration Through Exponentiated Lie Algebra provides reduced effect of scanner for cortex volumetry with atlas-based method in healthy subjects. *Neuroradiology*, 2013. 55(7): p. 869-875.
- [28]. Klein, A., et al., Evaluation of 14 nonlinear deformation algorithms applied to human brain MRI registration. *Neuroimage*, 2009. 46(3): p. 786-802.